International Journal of Advanced Mechanical Engineering.
ISSN 2250-3234 Volume 8, Number 1 (2018), pp. 205-212

http://www.ripublication.com

Performance Simulation of Passive Direct Methanol Fuel Cell

Dr. Ranjan K. Mallick[1*], Dr. Himanshu S. Moharana[2], Dr. Kailash Mohapatra[3], Dambarudhar Das[4] and Subhashree Pothal[5]

[1,3,4,5]Department of Mechanical Engineering, REC, Bhubaneswar,751024, India
[2]Department of Mechanical Engineering, HIT, Khordha, 752057, India
**E-mail: ranjan2mallick@gmail.com*

Abstract

In this work, a steady state and non-isothermal model is developed to simulate the performance of liquid feed passive Direct Methanol Fuel Cell (DMFC). The model is developed considering the heat and mass transfer effects. The model can serve as a prediction tool for estimating molar concentration of methanol, water and oxygen at each layer as well as temperature profiles. The developed model is validated with the experimental data.

***Keywords*:** DMFC, Mass transfer profile, temperature profile.

I. Introduction

The present energy scenario demands have given impetus to the development of alternative energy conversion technologies. Among these, direct methanol fuel cell (DMFC) has a prime position as a source to power portable electronic devices [1]. DMFC possesses high volumetric energy density, compact structure, easy refuelling and reliable operation [1-3]. The main characteristics of DMFC are its complex and intrinsically coupled transport and electrochemical phenomenon. Based on the mechanisms by which reactants reach the catalyst layers, DMFCs are classified into two types: active and passive. In active DMFC, the reactant flow is maintained by an external device (i.e. fan, blower etc.) for supplying them to reaction sites while in passive DMFC supply is solely by diffusion, capillary pressure and natural convection [4-7].With this in view, large numbers of extensive studies have been carried out by putting forth various analytical, semi-empirical and empirical models [8-12].

The modeling studies on passive DMFC's are a recent episode than that of active DMFC's. A. A. Kulikovsky [8] developed two-dimensional isothermal model on the effect of mass transfer and current density on reaction rates. Wang and Wang [9] developed two-phase, multi-component model and simulated the effect of methanol feed concentration on cell performance in detail. Garcia et al. [10]

developed one-dimensional, steady-state, isothermal model for predicting polarization curves. Chen and Zhao [11] simulated the effect of methanol concentration on performance by employing a one-dimensional, steady state model of passive DMFC. Chen et al. [12] developed two- dimensional, two-phase, steady-state and thermal model for passive DMFC to study the effect of important geometric design parameter.

In this work, a steady-state, one-dimensional, non-isothermal, thermal model is developed taking into consideration the mass and heat transport, electrochemical reactions in a passive DMFC. The model is used to predict the concentration profiles of methanol, water and oxygen throughout the cell. The model can be utilized for real-time simulation and diagnostic purposes with proper modifications.

II. Model development

A passive DMFC consists of a fuel reservoir (*fuelres*), anode current collector (ACC), anode diffusion layer (ADL), anode catalyst layer (ACL), polymer electrolyte membrane (M), cathode catalyst layer (CCL), cathode diffusion layer (CDL) and cathode current collector (CCC) as shown in Fig 1.

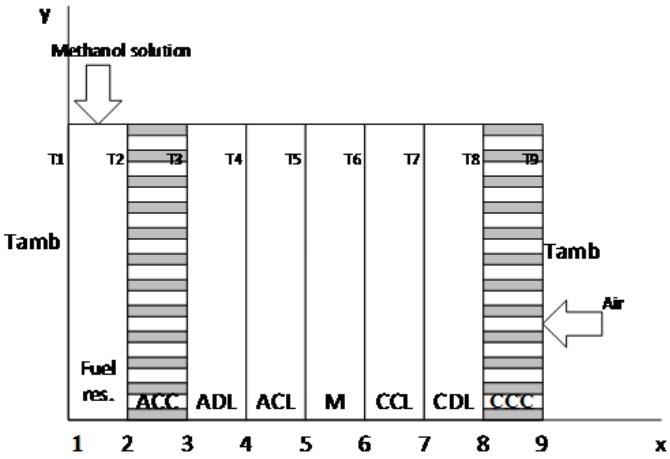

Fig 1: Schematic diagram of passive DMFC

The following simplifications and assumptions were made:

1. Steady state conditions are assumed for the fuel cell.
2. The mass and heat transport through the GDL and catalyst layers are predominantly by diffusion and are modeled as Fick's law and Fourier's law respectively.
3. The heat and mass transport in the fuel reservoir (from the bulk solution to ACC) i.e. anode side and from the cathode side is due to natural convection.
4. The temperatures at the wall of the cells are included in the solutions of the model equations.
5. The feed methanol concentration is constant throughout the FR.
6. The methanol is assumed to be in the liquid phase throughout the cell while gaseous water is considered at cathode.

7. The reactions in the catalyst layers are assumed to be supported by a homogeneous porous electrode.
8. The anode reaction mechanism is governed by kinetics proposed by Mayers and Newman while as the cathode side is governed by Tafel kinetics.
9. Joule heating is negligible

II.I Mass transport analysis in passive DMFC

In *fuelres*, methanol transport from the reservoir to the ACC is due to natural convection, $j_a^{AAP} = h_{mass}^{fuelres,a}(C_a^{bulk} - C_a^{AAP})$...(1)

Methanol diffusion is modelled by assuming Fick' model in ACC, ADL and ACL

$$j_m^n = -D_m^n \frac{dC_m^n}{dx} \text{...(2)}$$

Total methanol flux through the *fuelres*, ACC, ADL and ACL is same and given as follows: $j_{MeOH}^{AAP} = j_{MeOH}^{ACC} = j_{MeOH}^{ADL} = j_{MeOH}^{ACL} = \frac{I_{cell}}{6F} + j_{MeOH}^{Mem}$...(3)

The methanol flux through the membrane is given by,

$$j_{MeOH}^{Mem} = -D_{MeOH}^{Mem} \frac{dC_{MeOH}^{Mem}}{dx} + \xi_{MeOH} \frac{I_{cell}}{F} \text{...(4)}$$

Where j_{MeOH}^{Mem} represents methanol flux through membrane, D_{MeOH}^{Mem} represents diffusion coefficient of methanol through membrane, C is the molar concentration of methanol, ξ_{MeOH} is electro osmotic drag coefficient of methanol, I_{Cell} is cell current density and F represents the Faraday's constant.

Now, $j_{H_2O}^{AAP} = j_{H_2O}^{ACC} = j_{H_2O}^{ADL} = j_{H_2O}^{ACL} = (\alpha + 1)\frac{I_{cell}}{6F}$...(5) where α represents water transfer coefficient.

The water flux through the membrane is given by, $j_{H_2O}^{Mem} = -D_{H_2O}^{Mem} \frac{dC_{H_2O}^{Mem}}{dx} + n_d \frac{I_{cell}}{F}$...(6)

where $j_{H_2O}^{Mem}$ represents water flux through membrane, $D_{H_2O}^{Mem}$ represents diffusion coefficient of water through membrane, C is the molar concentration of water, n_d is electro osmotic drag coefficient of water.

The species diffusion is represented in CCL as,

$$j_b^{CCL} = -D_b^{CCL} \frac{dC_b^{CCL}}{dx} \text{...(7)}$$

The species diffusion in CDL and CCC is represented as, $j_e^f = -D_e^f \frac{dC_e^f}{dx}$...(8)

Also, water flux through CCL is due to WCO through membrane, water produced by methanol oxidation and oxygen reduction.

$$j_{H_2O}^{CCL} = -D_{H_2O}^{CCL} \frac{dC_{H_2O}^{CCL}}{dx} = \frac{\alpha I_{Cell}}{6F} + \frac{0.5 I_{Cell}}{F} + \frac{I_{MeOH}}{3F} \text{...(9)}$$

Oxygen transport from the ambient to the CCC is due to natural convection,

$j_{O_2}^{CCC} = h_{mass}^{CCC,O_2}(C_{O_2}^{atm} - C_{9,O_2}^{CCC})$...(10) where h_{mass}^{CCC,O_2} represents mass transfer coefficient of oxygen and C represents oxygen concentration.

II.II Reaction kinetics equation

The methanol oxidation can be given in terms of volumetric current density by Meyers-Newman equation :

$$j_A = aI_{0,ref}^{MeOH} \frac{kC_{MeOH}^{ACL}}{C_{MeOH}^{ACL} + \lambda \exp(\frac{\alpha_A \eta_A F}{RT_{ACL}})} \exp(\frac{\alpha_A \eta_A F}{RT_{ACL}}) \text{...(11)}$$

where a represents specific surface area of anode, $I_{0,ref}^{MeOH}$ represents exchange current density of methanol, k and λ are reaction constants, α_A represents anodic transfer coefficient, η_A represents anode overpotential , R represents gas constant, T_{ACL} is anode catalyst layer temperature.

The cell current density can be given by:

$$I_{cell} = \int_{ACL} j_A dx \text{...(12)}$$

The cathode reaction kinetics can be modeled by using Tafel kinetics

$$I_{cell} + I_{MeOH} = (1-s) I_{0,ref}^{O_2} \frac{C_{O_2}^{CCL}}{C_{O_2,ref}^{CCL}} \exp(\frac{\alpha_C \eta_C F}{RT_{CCL}}) \text{...(13)}$$

II.III Heat transport

The overall heat balance equation requires that the heat generated in the catalyst layers is the heat loss to the surroundings as $Q_{gen,ACL} + Q_{gen,CCL} = q_{anode} + q_{cathode}$...(14)

The equation for the temperature profiles in the ACL and CCL are given as:

$$\frac{d^2T}{dx^2} = \frac{Q_{gen,ACL}}{k_{ACL}\delta_{ACL}}...(15) \quad \text{and} \quad \frac{d^2T}{dx^2} = \frac{Q_{gen,CCL}}{k_{CCL}\delta_{CCL}}...(16)$$

The heat flux through the anode side (from ADL, ACC to AAP is given by

$$q_{anode} = k_i A_i \left(\frac{dT}{dx}\right)_i, i = ADL, ACC, AAP....(17)$$

Similarly, the heat flux through the cathode side (from CDL to CCC) is given by

$$q_{cathode} = -k_j A_j \left(\frac{dT}{dx}\right)_j, j = CDL, CCC....(18)$$

The heat transfer equation for AAP can be written as:

$$q_{anode} = q_{AAP} = h_{heat}^{fuelres} A_{AAP} (\Delta T)_{AAP}...(19)$$

h_{heat}^{AAP} represents heat transfer coefficient, A_{AAP} represents active area of AAP and

$(\Delta T)_{AAP} = T_{AAP/ACC} - T_{amb}$ is the temperature difference between AAP/ACC interface and the ambient temperature.

The heat transfer equation for CCC can be written as:

$$q_{cathode} = q_{CCC} = -h_{heat}^{CCC} A_{CCC} (\Delta T)_{CCC}....(20)$$

h_{heat}^{CCC} represents heat transfer coefficient, A_{CCC} represents active area of CCC and

$(\Delta T)_{CCP} = T_{CCC/amb} - T_{amb}$ is the temperature difference between CCC/*amb.* interface and the ambient temperature.

II.IV Cell performance

The cell voltage can be calculated by

$$V_{cell} = E_{cell} - \eta_A - \eta_C - I_{cell} R_{cell}....(21)$$

$$E_{cell} = U_{O_2} - U_{MeOH} + \Delta T(\frac{\partial E}{\partial T})....(22)$$

III. Experimental set-up

The active size of MEA was 50mm × 50mm. A Nafion® 115 membrane was hot-pressed between anode and cathode diffusion electrode at 135^0 C temperature and 8 MPa pressure for 3 minutes. The fuel reservoir of capacity 50.0mm x 50.0mm x 8.0mm was provided in the anode end plate.

The DC electronic load (Agilent Technologies, N3300A Mainframe & N3302A Module) was used to obtain the current-voltage (I-V) data points. Prior to this, activation of the MEA was done to recover sufficient hydration degree and to improve its proton conductivity. The cell temperature was measured by a K-type thermocouple.

IV. Results and discussions

The comparison of the experimental polarization curve and the power density curves and that of the model predictions for different methanol feed concentrations is shown in Fig. 2. It is apparent from the Fig. 2 that as the methanol concentration increases, the power density also increases. It is also found that both the voltage and power density curves show similar trends.

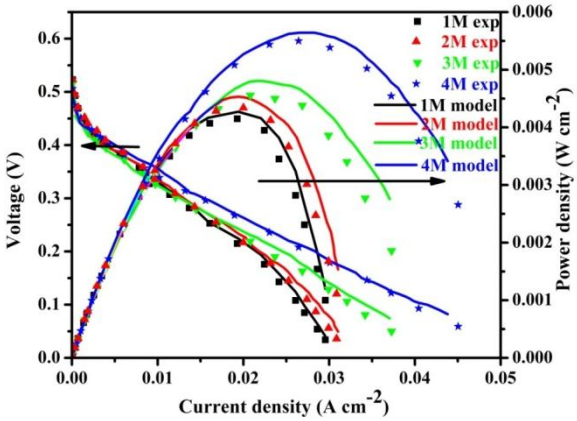

Fig. 2: Comparison of polarization curve and power density curve for different methanol concentrations

Fig.3(a) shows variation of species across different layers of the cell under 3 M methanol concentrations at current densities of 0.01, 0.03 and 0.05 A cm^{-2}.In fuel reservoir, natural convection mass transfer leads to decrease in the species concentration across the fuel reservoir upto ACC. Subsequently, the species concentration decreases across ADL by mass diffusion while by mass diffusion and electrochemical reactions in ACL. Further, species concentration across the membrane varies due to MCO and WCO and it decreases across CCL.

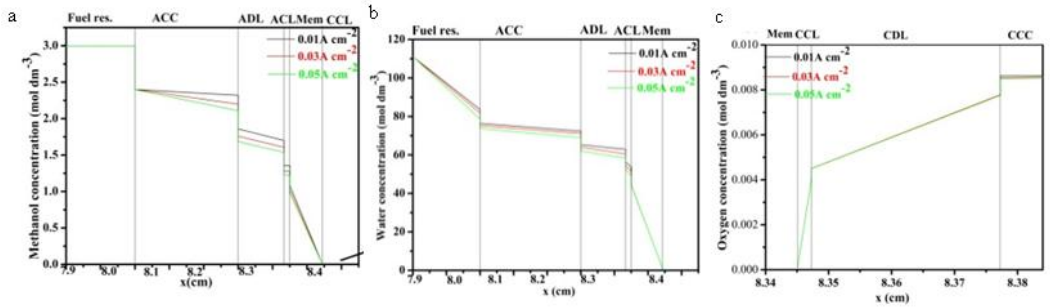

Fig. 3: (a) methanol concentration profile under; (b)water concentration profile; and (c) oxygen concentration profile under 3 m methanol concentrations at current densities of 0.01, 0.03 and 0.05 a cm^{-2}.

Fig. 3(b) shows the variation of water concentration across ACC, ADL and ACL at different current densities for 3M methanol concentration. Similarly, oxygen concentration variation across CCC is due to natural convection while mass diffusion is responsible for oxygen variation in CDL and CCL. Fig. 3 (c) shows the variation of oxygen concentration across CCC, CDL and CCL at different current densities for 3M methanol concentration.

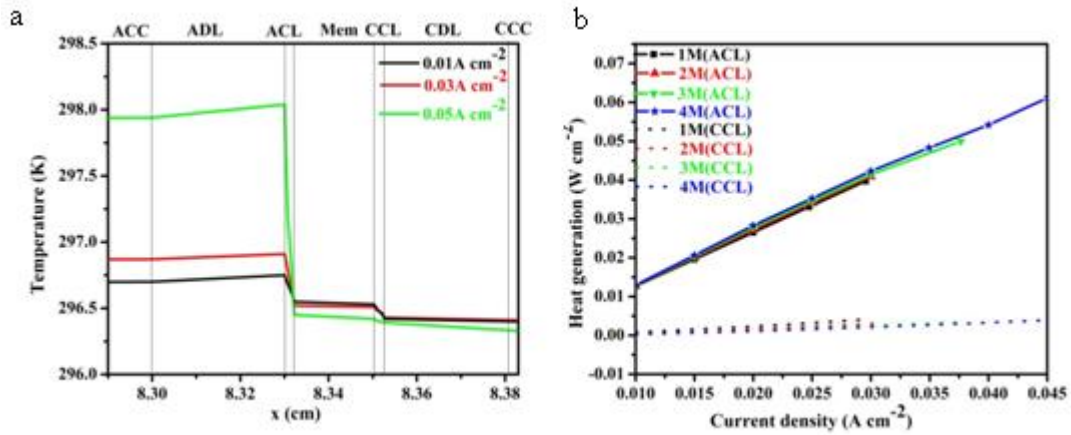

Fig. 4: (a) Temperature profile across the entire passive DMFC for different current densities at 3m concentration.(b) heat generation at ACL and CCL with respect to current density for different methanol concentration.

Fig. 4 shows the temperature profile in different layers encountered in passive DMFC. This is plotted for three current densities of 0.01, 0.03 and 0.05 A.cm^{-2} at 3M methanol concentration. The temperature encountered in ACL is higher than that at CCL at all current densities, and the ACL temperature increases with increase in current density. This is attributed to the fact that the heat generation in ACL is higher than that in CCL.

The heat generated due to anodic overpotential is more than the heat demanded from the endothermic reaction of methanol oxidation. The trend of temperature at various current densities can be explained for by the increase in

overpotential with increase in current density which increases the anodic overpotential heat generation. The heat generation variation with current density is shown in Fig. 4 (b) 5. It only confirms with the temperature profiles in that the heat generation at ACL is more than that at CCL for different methanol concentrations. Also, it can be seen from Fig. 4(b) that as the methanol concentration increases the heat generation in ACL increases while that in CCL decreases.

V. Conclusions

In this work, a simple one-dimensional, non-isothermal, steady state model is presented which can predict concentration profiles of various species, temperature profile and heat generation in catalyst layers under various conditions of important operating parameters. The model predictions are validated against the experimental data obtained as well as the published one. The trends in both are found to agree quite well.

References:

[1] Mallick, R., Thombre, S., Motghare, R., and Chillawar, R., 2016, "Analysis of the clamping effects on the passive direct methanol cell performance using electrochemical impedance spectroscopy," Electrochimica Acta, 215, pp. 150-161.

[2] Mallick, R., and Thombre, S., 2017, "Performance of passive DMFC with expanded metal mesh current collector," Electrochimica Acta, 243, pp. 299-309.

[3] Kothekar, K. P., Thombre, S. B., and Mallick, R.K., 2017, "Estimation of kinetic and electric parameters of liquid feed passive DMFCs," International Journal of Hydrogen Energy, 42, pp. 24358-24371.

[4] Mallick, R., Thombre, S. B., and Shrivastava, N., 2015, "A critical review of the current collector for passive direct methanol fuel cells," Journal of Power Sources, 285, pp. 510-529.

[5] Oliveira, V., Rangel, C., and Pinto, A, 2011, "One-dimensional and non-isothermal model for a passive DMFC," Journal of Power Sources, 196, pp. 8973– 8982

[6] Mallick, R., Thombre, S., and Shrivastava, N., 2016, "Vapor feed direct methanol fuel cells (DMFCs): A review," Renewable and Sustainable Energy Reviews, 56, pp. 51-74.

[7] Kamaruddin, M., Kamarudin, S., Daud, W., and Masdar, M., 2013, "An overview of fuel management in direct methanol fuel cells," Renew. Sustain. Energy Rev., 24, pp. 557-565.

[8] Kulikovsky, A., 2000, "Two-dimensional numerical modeling of a direct methanol fuel cell," Journal of Applied Electrochemistry, 30, pp. 1005-1014.

[9] Wang, Z., and Wang, C., 2000, "Mathematical Modeling of Liquid-Feed Direct Methanol Fuel Cells," Journal of The Electrochemical Society, 150 (4), pp. A508-A519.

[10] García, B., Sethuraman, V., Weidner, J., White, R., and Dougal, R., 2004, "Mathematical Model of a Direct Methanol Fuel Cell," Journal of Fuel Cell Science and Technology, 1, pp. 43-48.

[11] Chen, R., and Zhao, T., 2005, "Mathematical modeling of a passive-feed DMFC with heat transfer effect," Journal of Power Sources, 152, pp. 122–130.

[12] Chen, R., Zhao, T., Yang, W., and Xu, C., 2008, "Two-dimensional two-phase thermal model for passive direct methanol fuel cells," Journal of Power Sources, 175, pp. 276–287.